Synthesis and Reactivity in Inorganic, Metal-Organic, and Nano-Metal Chemistry, 42:823–832, 2012

ISSN: 1553-3174 print / 1553-3182 online
DOI: 10.1080/15533174.2011.618474

Taylor & Francis
Taylor & Francis Group

Synthesis, Characterization, Reactivity, and Antibacterial Studies of Triethylammonium-3-silatranylpropyldithiocarbamate, Spectroscopic, and Quantum Mechanical Studies of 3-(Silatranyl)propylammonium Chloride

Raghubir Singh,[1] Jugal Kishore Puri,[2] Varinder Kaur Chahal,[2] Raj Pal Sharma,[2] Sabeta Kohli,[3] Rajni Kant,[3] and Baljinder Singh Gill[4]

[1]*Department of Applied Sciences, Sachdeva Engineering College for Girls, Gharuan, Mohali, India*
[2]*Department of Chemistry, Panjab University, Chandigarh, India*
[3]*Department of Physics, University of Jammu, Jammu Tawi, India*
[4]*Department of Biotechnology, Panjab University, Chandigarh, India*

3-aminopropylsilatrane (1) was crystallized as its hydrochloride salt, 3-(silatranyl)propylammonium chloride (2), which was confirmed by spectroscopic and X-ray diffraction studies. Single-crystal X-ray data revealed orthorhombic crystal system (space group = $P2_12_12_1$) with three molecules packed in an asymmetric unit cell. Herein, a special emphasis on the experimental and computational methods is given to study the geometric and spectroscopic parameters of 3-(silatranyl)propylammonium chloride (2). The scaled values of vibrational frequencies were obtained by using different basis sets. To study the reactivity of 1 toward nucleophilic addition reactions, it was treated with CS_2 in the presence of triethylamine, which resulted in a novel silatrane, triethylammonium-3-silatranylpropyldithiocarbamate (4). Due to its ability to act as bidentate ligand (L), reactivity of 4 was studied by reacting it with Cu(II), Co(II), Ni(II), and Pd(II) metal salts. The composition, nature of bonding, and geometry of complexes have been deduced from elemental analysis, and infrared and electronic spectral studies. The electronic and vibrational absorption spectra of these complexes indicated the formation of Cu(II), Ni(II), and Pd(II) complexes in 1: 2 ratio but 1:3 ratio (M:L) in Co(II) complex. Compound 4 is found to be moderately active against some bacteria such as *Esherichia coli, Bacillus subtillus*, and *Staphylococcus aureus*.

Keywords 3-aminopropylsilatrane, dithiocarbamate, DFT, HF, metal complexes, Triethylammonium-3-silatranylpropyl-dithiocarbamate

Received 4 January 2011; accepted 21 August 2011.

Raghubir Singh is thankful to UGC, New Delhi for providing financial support [F-4–1/2006 (BSR)]. Rajni Kant is thankful to Ministry of Science and Technology, Govt. of India for funding under major research [project No. SR/S2/CMP-47].

Address correspondence to Jugal Kishore Puri, Department of Chemistry, Panjab University, Chandigarh 160 014, India. E-mail: prof_jkpuri@yahoo.com

INTRODUCTION

Silatranes have captured extensive interest of scientists due to their unusual structure, biological properties and applications in the field of material sciences.[1–4] A variety of derivatives of 3-aminopropylsilatrane have been prepared in the past due to reactivity of $–NH_2$ group with various reagents such as alkyl halides, aryl halides, phosphoramide-tegafur derivatives, phosphoryl halides, and dicyclohexylcarbodiimide.[4,5] It is well known that silatranes derived from 3-aminopropylsilatrane such as 1-arylaminopropylsilatranes (aryl = chlorophenyl and nitrophenyl) and 1-arylsulfonylaminopropylsilatranes exhibit significant antimicrobial activity against gram-negative and gram-positive bacteria.[6,7] In addition, 3-formylchromoniminopropylsilatrane and its metal complexes showed antibacterial activity against *K. pneumoniae*, *S. aureus*, *E. coli*, and *B. subtilis*.[8]

Prompted by favorable research work and our interest in the field of organosilicon complexes,[9–11] we worked on **1** in order to explore its reactivity. In the present contribution, the molecular structure of 3-(silatranyl)propylammonium chloride (**2**), established by X-ray crystallography and its comparison with theoretical studies, is reported. The optimization of structure was done by using computational studies such as Density Functional Theory (DFT) and Hartree-Fock theory with different basis sets.

Previously, we reported one-pot synthesis of 3-isothiocyanatopropylsilatrane in which CS_2 was reacted with **1** to form its dithiocarbamic acid, followed by addition of dicyclohexylcarbodiimide.[5] In the presented work, dithiocarbamate of **1** (derivatives of dithiocarbamic acid) was synthesized by addition of carbon disulphide in the presence of triethylamine, which resulted in the formation of [3-(2,8,9-trioxa-5-aza-1-silabicyclo[3.3.3]undec-1-yl)-propyl]-dithiocarbamic acid (**3**). As

the compound was insoluble in common organic solvents, its triethylammonium salt (**4**) was prepared for characterization. Since dithiocarbamates are known to be very good chelating agents and can stabilize a wide range of oxidation states of different metal ions due to their unique property to remain intact under a variety of reaction conditions.[12,13] Therefore, different metal complexes (**5**–**8**) have been prepared to study the reactivity of **4** as coordinating ligand. Compound **4** also shows antibacterial activity against *Esherichia coli*, *Bacillus subtillus*, and *Staphylococcus aureus*.

EXPERIMENTAL

Materials and Methods

All the syntheses were carried out under a dry nitrogen atmosphere using vacuum glassline. Organic solvents used were dried and purified according to standard procedures and stored under nitrogen. 3-aminopropyl(triethoxy)silane (Aldrich, St. Louis, USA), triethanolamine (Merck, India), and carbon disulphide (Qualigens, India) were used as such without any further purification. Triethylamine (Qualigens, India) was kept over KOH for several days and distilled prior to use. Infrared spectra were routinely obtained as Nujol thin films or KBr pellets on a Perkin-Elmer RX-I FT IR spectrophotometer (USA). Mass spectral measurements (ESI source with capillary voltage, 2500 V) were carried out on a VG Analytical (70-S) spectrometer. C, H, and N analyses were obtained on a Perkin-Elmer Model 2400 CHN elemental analyzer (USA). S and Si were estimated by gravimetric methods. The solution NMR spectra were recorded at 25°C on Jeol FT NMR (AL 300 M Hz) and Bruker Avance II FT NMR (AL 400 MHz) spectrometers (USA) (^{1}H, ^{13}C) using $CDCl_3$ as the solvent. Chemical shifts in ppm were determined relative to internal $CDCl_3$ and external tetramethylsilane (TMS).

X-Ray Crystallography

Three-dimensional intensity data were collected by using X'calibur single-crystal X-ray diffractometer with CCD camera using MoKα radiation ($\lambda = 0.71073$ Å). CrysAlis^{Pro} software was employed for data collection, data reduction, and space group determination.[14] The structure was solved by direct methods using SHELXS86 software (England). Full-matrix least-squares refinement of the non-hydrogen atoms with isotropic temperature factors was carried out using SHELXL97 (England). Subsequent cycles of refinement yielded final R-factor of 0.0548. All principle crystallographic parameters and X-ray diffraction characteristics are summarized in Table 1.

TABLE 1
X-ray crystal data and structure refinement of **2**

Empirical formula	$(C_9H_{21}ClN_2O_3Si)_3$
Formula weight	806.45
Temperature	293(2) K
Diffractometer used	X'calibur Single crystal diffractometer
Radiation used, wavelength	MoKα, 0.71073 Å
Crystal system, space group	Orthorhombic, $P2_12_12_1$
Unit cell dimensions (Å)	a = 11.3331(7), b = 17.9935(10), c = 19.7443(9); $\alpha = 90^\circ$, $\beta = 90^\circ$, $\gamma = 90^\circ$
Volume	4026.3(4) Å^3
Z	12 (three molecules in a unit cell)
Density (calculated)	1.330 Mg/m^3
F(000)	1728
Crystal size	0.30 × 0.22 × 0.20 mm
Theta range for data collection	3.07 to 32.39°
Index ranges	$-16 \le h \le 13$, $-26 \le k \le 19$, $-28 \le l \le 29$
Reflections collected	17158
Independent reflections	11291 [R(int) = 0.0306]
Refinement method	Full matrix least squares on F^2
Data / restraints / parameters	11291/ 0 / 470
Goodness-of-fit on F^2	0.957
Final R indices, 1631 reflections [$I > 2\sigma(I)$]	$R_1 = 0.0548$, $wR_2 = 0.1194$
R indices (all data)	$R_1 = 0.0942$, $wR_2 = 0.1306$
Absorption corrections	None

Theoretical Studies

Quantum mechanical calculations were carried out by using GAUSSIAN 03 series of programs (USA). Geometries were fully optimized at both the Restricted Hartree-Fock (RHF) and DFT level, using Becke's three-parameter hybrid exchange functional and the correlation functional of Lee, Yang, and Parr (B3LYP) with 3–21G*(d), 6–31+G*(d), and 6–311+G*(d) basis sets.

Assessment of Antibacterial Activity

Disc diffusion method

Antimicrobial activity was determined by disk diffusion method. In this technique, the filter paper (Whatman no. 1) sterile disc of 5 mm diameter impregnated with test compounds (2 mg/mL of DMSO) were placed in nutrient agar plate at 37°C for 12 h. The inhibition zones around the dried impregnated disks were measured after 12 h.

Test microorganism

Test isolates were taken from the MTCC (Microbial Type Culture Collection) at the Institute of Microbial Technology (IMTECH), Chandigarh, India, and included *Escherichia coli, Bacillus subtillus*, and *Staphylococcus aureus.*

Synthesis of 3-aminopropylsilatrane (1)

The starting material **1** was synthesized according to the method reported in literature.[15] 3-aminopropyl(triethoxy) silane (5.00 g, 22.5 mmol) was added at room temperature to triethanolamine (3.36 g, 22.5 mmol) in a two-necked flask which was fitted with a Dean Stark trap. The resulting mixture was refluxed to remove ethanol formed during the reaction. After the complete removal of ethanol, the reaction mixture was kept in refrigerator for 5 h, when white solid was obtained. Dry hexane was added, and contents were stirred for 30 min, filtered, and dried under vacuum.

Synthesis of Triethylammonium-3-silatranylpropyldithiocarbamate (4)

3-aminopropylsilatrane (2 g, 8.62 mmol) in dry THF (50 mL) was taken in a 100 mL two-necked round bottom flask and to this solution 2 mL of CS_2 was added dropwise with constant stirring. The reaction mixture was cooled in an ice salt mixture. A light yellow solid separated out immediately. The contents were stirred for 30 min. Then, triethylamine (1 mL, 8.62 mmol) was added dropwise with constant stirring. Initially, yellow solid was dissolved but reappeared after 10 min. The reaction mixture was stirred for 5 h at room temperature. The crude product was filtered, washed with THF (2×10 mL), and dried under vacuum. M.Pt: 142–145°C. Yield: 3.13 g, 90%. Anal. Calcd. for $C_{16}H_{35}N_3O_3S_2Si$ (%): C, 46.91; H, 8.61; N, 10.26; S, 15.65; Si, 6.86. Found: C, 46.70; H, 7.98; N, 10.01; S, 14.78; Si, 6.02. IR (KBr pellet, cm^{-1}): 3356, 3181 s ν (N-H), 2926, 2871 vs, ν (C-H), 1630 m, ν (C = S), 1471 vs, ν (C-N), 1360 m, 1325 m, ω (CH_2N), 1278 m, ω (CH_2O), 1185 m, τ (CH_2O), 1121 s, 1096 s, 987 s, 938 s, ν (Si-O-C-C), 760 s, δ_{as} (SiO_3), 716 vs, 613 m, δ (C = S), 645 m, δ_s (SiO_3), ν_s (Si-C), 584 m ν (Si←N), 472 m, δ (NCS). ^{1}H NMR (400 MHz, $CDCl_3$, ppm): δ 3.75–3.78 (t, 6H, OCH_2), 2.80–2.83 (t, 6H, NCH_2), 0.431–0.455 (t, 2H, CH_2Si), 1.66–1.70 (m, 2H, CCH_2C), 3.50–3.51 (t, 2H, CH_2NCS_2), 1.35–1.39 (t, 9H, CCH_3), 3.22–3.27 (q, 6H, $NHC\boldsymbol{H}_2$), 8.00 (s, 1H, NH), 8.59 (s, 1H, NH). ^{13}C NMR (100.62 MHz, $CDCl_3$, ppm): δ 209.41 (NCS_2), 55.33 (OCH_2), 49.37 ($\boldsymbol{C}H_2NC$), 48.99 (NCH_2), 43.75 ($NHCH_2$), 21.78 ($C\boldsymbol{C}H_2C$), 11.51 ($SiCH_2$), 6.91 (CH_3). EI-MS: *m/z* (relative abundance,%): 233.5 (23.01), 192.5 (29.51), 174.5 (14.68), 150.5 (1.65), 102.5 (100).

Synthesis of Co Complex (5)

To a well-stirred solution of **4** (0.5 g, 1.22 mmol) dissolved in acetonitrile, anhydrous $CoCl_2$ (0.053 g, 0.41 mmol) was added. Green coloration appeared immediately. The contents were stirred for 5 h at room temperature. The solution became dark green during the course of reaction, which indicated complexation of cobalt with **3**. The contents were filtered under vacuum and solvent was evaporated near to dryness. Hexane was added and the contents were stirred for 30 min. Green solid was filtered under vacuum and dried. Anal. Calcd. for $C_{30}H_{60}CoN_6O_9S_6Si_3$: C, 36.60; H, 6.14; N, 8.54; Si, 8.56; Found: C, 35.99; H, 5.60; N, 8.05; Si, 8.02; IR: cm^{-1}, 1509 vs ν (C-N), 1010 vs ν (C-S), 581 w ν (Si-N), 477 s ν (Co-S); UV-Vis: nm, 655, 322, 245.

Synthesis of Cu Complex (6)

To a well-stirred solution of **4** (0.5 g, 1.22 mmol) dissolved in acetonitrile, anhydrous $CuCl_2$ (0.08 g, 0.61 mmol) was added. The contents were stirred for 5 h at room temperature. A brown-colored solution was obtained, which indicated complexation of copper with **3**. The solution was filtered under vacuum, solvent was evaporated near to dryness, and hexane was added. The contents were stirred for 30 min, filtered, and brown solid was dried under vacuum. Anal. Calcd. for $C_{20}H_{40}CuN_4O_6S_4Si_2$**:** C, 35.30; H, 5.92; N, 8.23; Si, 8.25; Found: C, 32.83; H, 5.08; N, 8.13; Si, 7.67; IR: cm^{-1}, 1528 vs ν (C-N), 1011 vs ν (C-S), 581 w ν (Si-N), 459 s ν (Cu-S); UV-Vis: nm, 431, 370.

Synthesis of Ni Complex (7)

In dry acetonitrile, **4** (0.5 g, 1.22 mmol) was taken in a round-bottomed flask and nickel chloride (0.08 g, 0.61 mmol) was added. Light green color appeared and the contents were stirred for 5 h at room temperature. The precipitated solid was filtered and solvent was evaporated when green solid was obtained. Hexane was added, stirred for 30 min, filtered, and dried under vacuum. Anal. Calcd. for $C_{20}H_{40}N_4NiO_6S_4Si_2$: C, 35.55; H, 5.97; N, 8.29; Si, 8.31; Found: C, 34.50; H, 5.10; N, 7.94; Si, 7.98; IR: cm^{-1}, 1543 vs ν (C-N), 1012 vs ν (C-S), 581 w ν (Si-N), 455 s ν (Ni-S); UV-Vis: nm, 380, 324.

Synthesis of Pd Complex (8)

To the stirred solution of **4** (0.5 g, 1.22 mmol) in dry acetonitrile, palladium chloride (0.12 g, 0.61 mmol) was added. The mixture turned brown upon stirring for 5 h. The contents were filtered and reduced under vacuum. Hexane was added to obtain a brown solid, which was filtered, washed with 15 mL of hexane. The solid was dried under vacuum and analyzed with spectroscopic methods. Anal. Calcd. for $C_{20}H_{40}N_4O_6PdS_4Si_2$: C, 33.21; H, 5.57; N, 7.74; Si, 7.76; Found: C, 33.01; H, 5.33; N, 7.01; Si, 7.02; IR: cm^{-1}, 1547 vs ν (C-N), 1012 vs ν (C-S), 581 w ν (Si-N), 446 s ν (Pd-S); UV-Vis: nm, 296.

RESULTS AND DISCUSSION

Synthesis

Investigation of spectroscopic data and crystallographic details of crystals evidenced the formation of 1·HCl. It was concluded from literature survey that **1** undergoes a photochemical reaction in dichloromethane to form its ammonium salt. In the past, Balsells et al.[16] discussed photochemical behavior of aliphatic amines in dichloromethane and suggested the formation of hydrochlorides of different primary amines in amine-dichloromethane mixture. A proposed mechanism for the formation of **2** from mixture of **1** in dichloromethane is given in Scheme 1.

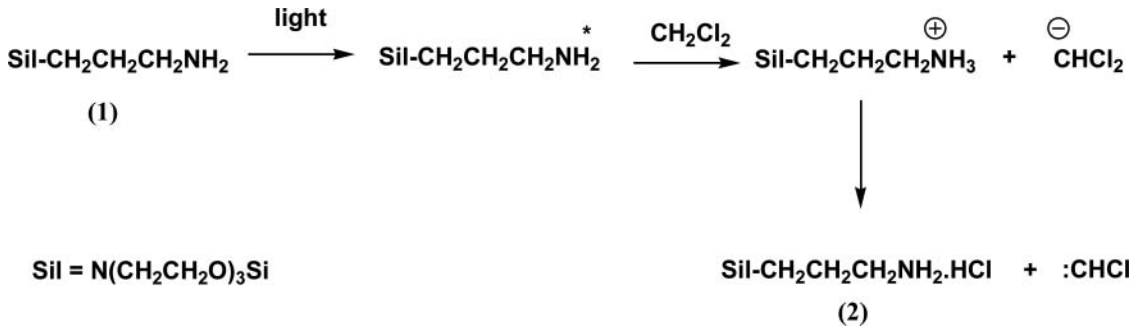

SCH. 1.

The previously mentioned mechanism involves the photoexcitation of **1** in which it is elevated to higher energy excited state (S_1). The reaction proceeds via n-σ^* transition generating diradical or zwitterionic state. This excited molecule then abstracts hydrogen from the solvent, resulting in the formation of ammonium ion, which facilitates the transfer of Cl^- ion with simultaneous generation of carbene.

The participation of aminopropylsilatrane (**1**) in nucleophilic addition reactions was confirmed by treating it with CS_2 (1:1) followed by addition of triethylamine, which resulted in the formation of **4** (Scheme 2). From the previous reports, it was found that Si-N bond undergoes cleavage on addition of electrophiles resulting in the quaternization of N atom.[17] Herein, it is observed that addition of CS_2 results in the formation of new silatrane without affecting transannular Si-N bond. The presence of S atoms makes **4** very interesting, as it can display variable coordination modes. Different metal ions such as Cu, Co, Ni, and Pd form different metal complexes with **4**. Among these metal ions, Cu(II), Pd(II), and Ni(II) form 1:2 complexes, whereas Co(II) forms a 1:3 (M:L) complex.

X-Ray Crystal Structure

Crystals of **2** were obtained by slow evaporation of solvent from saturated solution of **1** in dichloromethane and dichloromethane-hexane mixture. ORTEP view of asymmetric unit along with atomic labeling (thermal ellipsoids are drawn at 50% probability) is shown in Figure 1. The bridging elements in rings are labeled as Ring R_1 (N1, Si, O3, C6, C5), Ring R_2 (N1, Si, O1, C1, C2), and Ring R_3 (N1, Si, O2, C3, C4). The corresponding atoms in molecule I and III have been represented by ′ and ″, respectively. The molecules I, II, and III comprise three five-membered rings with Si-N as a common (fused) bond. Si-N bond distances in case of all the three asymmetric molecules (2.113(2) Å, 2.190(3) Å, and 2.116(3) Å) are in agreement with the structural trends found for silatranes. Selected bond lengths and angles for **2** are summarized in Table 2.

In the asymmetric unit, there exist three independent molecules. The molecules I and II adopt *anticlinal* conformation **A** in which $CH_2CH_2CH_2NH_3^+$ moiety is oriented in a zig-zag fashion (Figure 2). Whereas molecule III acquired conformation **B** in which NH_3^+ group of chain is present on same side of $CH_2(\alpha)$ (i.e., the chain is not in a zig-zag fashion). The molecule III stays in this conformation

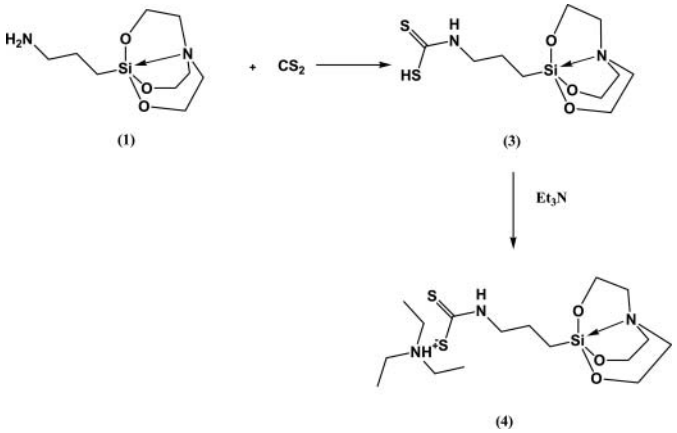

SCH. 2.

TABLE 2
Selected bond lengths (Å) and angles (°) of I, II, and III

Bond length, Bond angles	Molecule I	Molecule II	Molecule III
O(1)-Si (av)	1.670 (2)	1.653 (3)	1.671 (2)
Si-C(7)	1.888 (3)	1.873 (3)	1.868 (3)
Si-N(1)	2.113 (2)	2.190 (3)	2.116 (3)
N(1)-C(4) (av)	1.461 (5)	1.463 (5)	1.393 (6)
C(8)-C(7)	1.520 (4)	1.521 (5)	1.517 (4)
C(8)-C(9)	1.522 (4)	1.509 (4)	1.514 (5)
N(2)-C(9)	1.481 (5)	1.484 (4)	1.496 (5)
O(2)-Si-O(3) (av)	118.66 (1)	117.30 (2)	119.35 (1)
O(2)-Si-C(7) (av)	96.53 (1)	97.55 (1)	96.63 (1)
C(7)-Si-N(1)	179.08 (1)	179.29 (2)	178.41 (1)
C(4)-N(1)-C(5)	113.5 (3)	113.0 (3)	112.3 (7)
C(7)-C(8)-C(9)	113.6 (2)	112.3 (3)	113.3 (3)
C(8)-C(7)-Si	114.2 (2)	112.2 (2)	117.0 (2)
N(2)-C(9)-C(8)	109.9 (3)	109.7 (3)	112.2 (3)

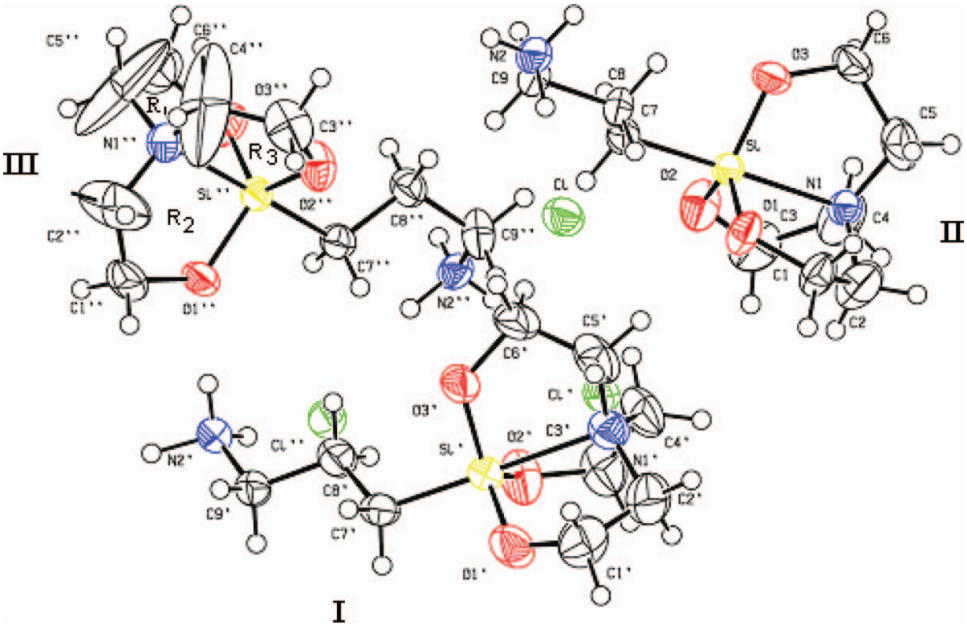

FIG. 1. Perspective view of asymmetric unit cell with atomic numbering scheme (thermal ellipsoids drawn at 50% probability) (color figure available online).

presumably due to extra stabilization caused by N2″-H10G. . .$Cl^{-\prime\prime}$ interaction, which forced CH_2-NH_3^+ bond to rotate toward Cl^-. The molecular arrangement of this kind is quite favorable in the formation of a trifurcated Cl^- ion interaction.

Unit cell packing revealed the arrangement of molecules in a zig-zag fashion along the b-direction in the bc-plane. The lattice is further stabilized by some additional hydrogen bonded interactions (between oxygen atoms of silatrane moiety and hydrogen atom of NH_3^+ as well as $CH_2(\gamma)$). In view of the multiple molecule phenomena as exhibited by the asymmetric unit, it is difficult to depict hydrogen-bonded network with clarity. However, the plot (Figure 3) clearly displays network of few intra- and intermolecular hydrogen bonds of the type C-H. . .O, C-H. . .Cl, N-H. . .Cl and N-H. . .O.

The carbon atoms C5, C2″, and C5″, which are linked to nitrogen (N1, N1ã), have large thermal amplitude and hence are found disordered. Asymmetry parameter calculations as proposed by Duax and Norton for molecule I are: ring R_1 (ΔC_2 = 14.498, ΔC_s = 5.4712), ring R_2 (ΔC_2 = 11.981, ΔC_s = 5.0601), and ring R_3 (ΔC_2 = 11.865, ΔC_s = 6.196). Corresponding values for molecules II and III are: ring R_1 (ΔC_2 = 2.5075, ΔC_s = 5.4712; ΔC_2 = 3.637, ΔC_s = 1.5578), for ring R_2 (ΔC_2 = 2.2000, ΔC_s = 13.5889; ΔC_2 = 6.5800, ΔC_s = 0.9398), and for ring R_3 (ΔC_2 = 2.1066, ΔC_s = 15.424; ΔC_2 = 6.823, ΔC_s = 0.4716), respectively[18,19]

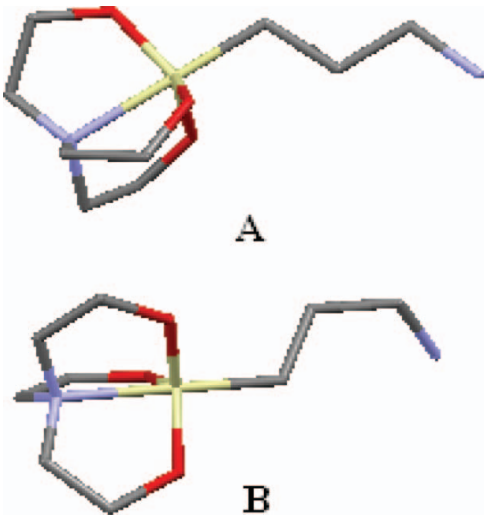

FIG. 2. Conformation of independent molecules; A belongs to I and II, B belongs to molecule III (color figure available online).

Theoretical Studies

The geometry of **2** was optimized and values for various bond lengths and bond angles optimized by DFT/B3LYP and HF methods with different basis sets such as 3–21G*(d), 6–31+G*(d), and 6–311+G*(d) are given in Table 3. In theoretical calculations, the molecule is considered in gaseous state; therefore, crystal effects are found to be absent. Some bond lengths and angles such as the Si-C bond length computed with DFT/3–21G*(d) were almost similar with X-ray crystallographic data but Si-N, Si-O (av.), and N-C bond lengths deviate from the experimental values. The changes observed in bond lengths might be because of crystal packing forces in the solid state.

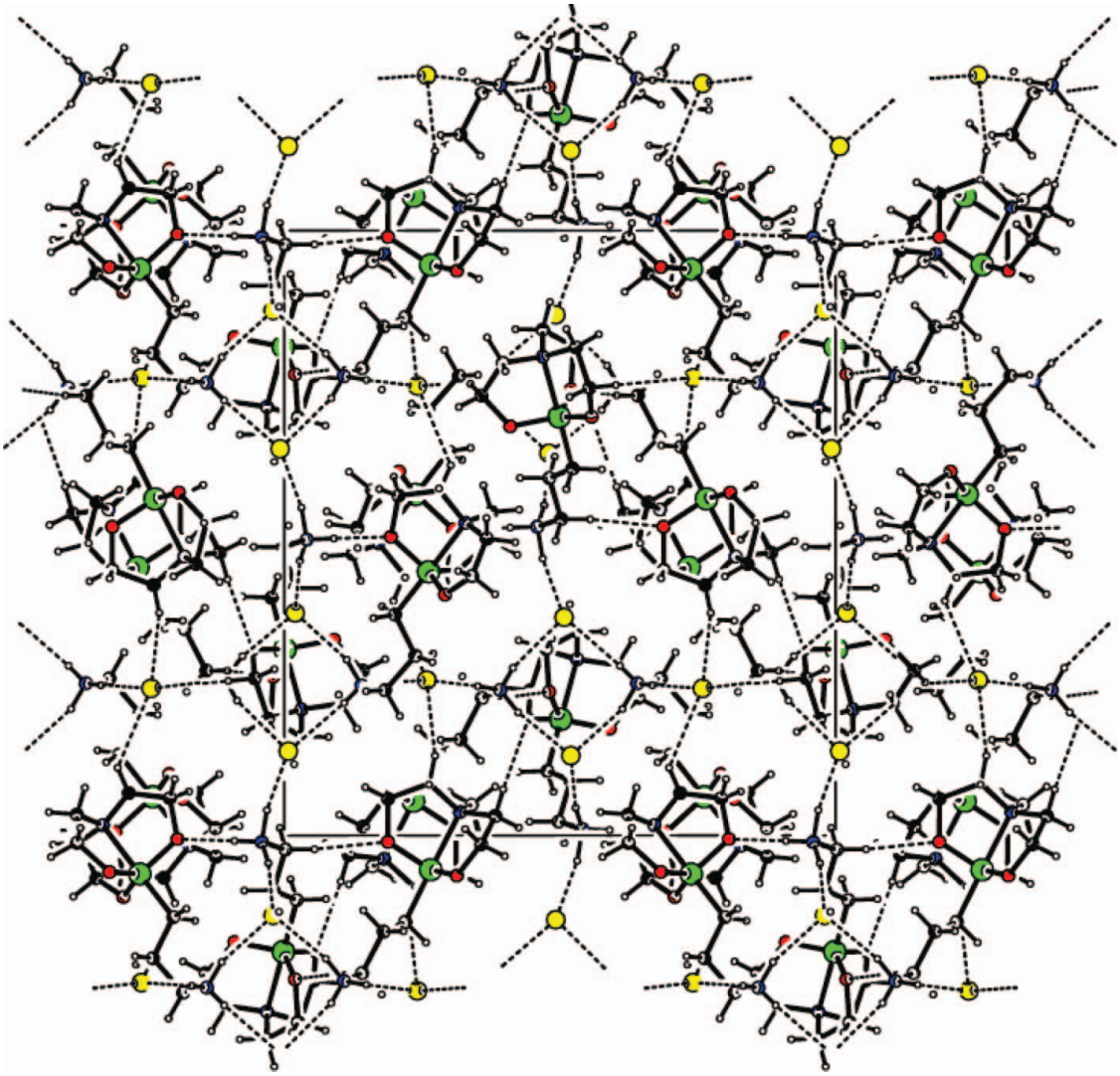

FIG. 3. Unit cell molecular packing diagram showing hydrogen-bonding network along *b* direction in *bc* plane (color figure available online).

Spectroscopic Studies

IR spectroscopy

Theoretical values for fundamental vibrational frequencies optimized by HF and DFT/B3LYP using 6–31+G*(d) basis sets are given in Table 4 and are compared with experimental IR frequencies. Comparison of frequencies calculated at the DFT method using different basis sets with experimental values revealed that B3LYP method is in good agreement with experimental observation. The HF and DFT methods showed symmetric and asymmetric stretching for methylene groups in the region of 2900–3000 cm^{-1}, which are supported by experimental results. Theoretically, C-H stretching frequency for O-CH_2 is found to be higher than N-CH_2, which is observed experimentally at 2934.6 and 2875.9 cm^{-1}.

Generally, ν (C–N) absorption in silatranes is observed in the range of 800–900 cm^{-1}. In this molecule, position of the ν (C–N) absorption is also observed at 863 cm^{-1}, which lies in the range 833–967 cm^{-1} obtained from theoretical calculations. Two bands observed at 1124 cm^{-1} and 971.5 cm^{-1} for symmetric and asymmetric stretching of NC_3 fragment of silatrane ring are displayed in the range of 1055–1160 cm^{-1} and 976–972 cm^{-1}, respectively, by theoretical studies. In addition, Si–N stretching frequency is of great interest as it indicates hypervalency of silicon. Theoretically, this absorption band along with silatranyl skeletal vibrations is obtained in the region 570–600 cm^{-1} that is in accordance with experimental data (i.e., at 583.4 cm^{-1}). In the present studies, Si-O asymmetric and symmetric stretching is observed in the region of 1110–1170 cm^{-1} and 740–760 cm^{-1}, respectively. In addition, investigation of silatranes for structural fragment of Si-O-C-C was characterized by typical frequencies appearing in the region of 1480–575 cm^{-1}. Therefore, experimental data of this molecule are found to be consistent with theoretical data.

TABLE 3
Selected bond lengths, bond angles, and other parameters optimized by DFT and HF studies of **2**

	HF			DFT		
Parameters	3–21G*(d)	6–31+G*(d)	6–311+G*(d)	3–21G*(d)	6–31+G*(d)	6–311+G*(d)
Total energy; a.u	−1427.936	−1435.074	−1435.263	−1433.479	−1440.625	−1440.832
N(1)→Si	2.615	2.594	2.616	2.398	2.503	2.534
Si-C(7)	1.866	1.876	1.871	1.879	1.883	1.877
Si-O av.	1.649	1.646	1.641	1.692	1.679	1.674
N(1)-C(2,4,6) av.	1.468	1.448	1.448	1.490	1.462	1.460
N(2)-C(9)	1.518	1.487	1.486	1.519	1.492	1.491
NH_3^+-Cl^-	2.936	2.939	2.936	2.875	2.868	2.872
N(2)-C(9)-C(8)	111.75	112.59	112.72	112.70	113.71	113.69
C(9)-C(8)-C(7)	113.78	114.50	114.51	113.90	114.57	114.53
C(8)-C(7)-Si	112.33	114.51	114.60	113.05	114.93	114.88
O(1)-Si(1)-O(2)	113.69	114.31	113.94	117.05	116.12	115.71
O(2)-Si(1)-O(3)	113.15	113.81	113.43	116.69	115.51	115.08
O(3)-Si(1)-O(1)	112.70	113.48	113.15	116.12	115.38	114.91
C(2)-N(1)-C(4)	117.46	117.83	118.01	115.38	116.88	117.17
C(4)-N(1)-C(6)	117.45	117.79	117.98	115.37	116.86	117.15
C(6)-N(1)-C(2)	117.39	117.79	117.97	115.31	116.85	117.14

IR spectra of **4** exhibit absorption bands characteristic of the dithiocarbamate and silatranyl moiety. These bands were assigned by comparison with the spectra of starting materials and literature data.[20–22] Strong bands present in the regions 1400–1150 cm^{-1} are assigned to asymmetric and symmetric deformations of CH_2 group, respectively. Si–O stretching vibration is assigned to the bands present in 1100–1080 cm^{-1} region. A weak band observed in the region 480–450 cm^{-1} is attributed to stretching vibrations of the M–S.

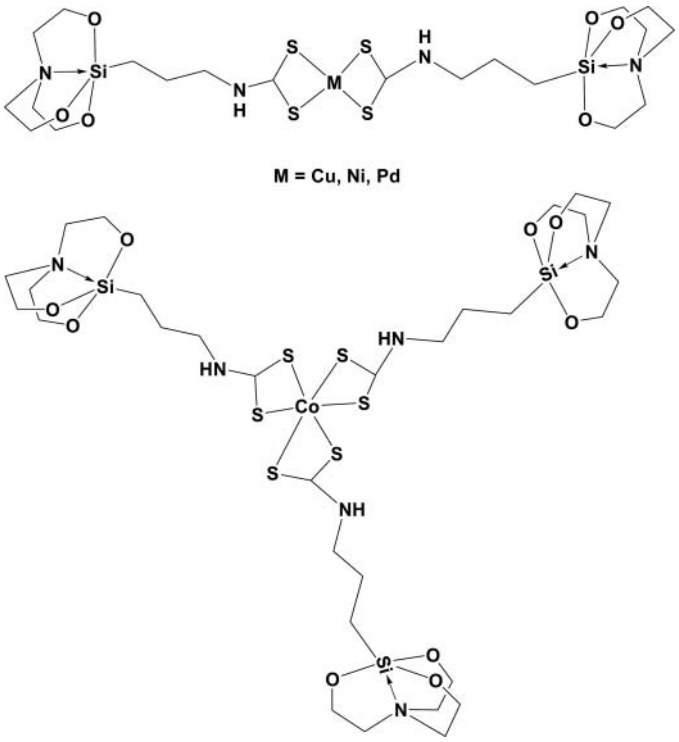

FIG. 4. Expected structures of complexes **5**–**8**.

C–S stretching frequencies are of great interest, as these can be used to differentiate between mono- and bidentate modes of binding of dithiocarbamate ligands. The absorption frequencies for C-S and C = S can be observed in the region of 1350–1250 cm^{-1} and 1680–1470 cm^{-1}, respectively. In these studies, C = S stretching was observed at 1653 cm^{-1} in **4**, which is absent in metal complexes, indicating the absence of double bond. In metal complexes (**5–8**), presence of only one band in the region of 1061–980 cm^{-1} for ν(CSS) mode, suggests a symmetrical bonding of bidentate dithiocarbamate moiety. In the free dithiocarbamate (**4**), C-N band was observed at 1471 cm^{-1}, which was shifted in the range of 1550–1509 cm^{-1} after coordination with metals indicating the presence of partial double bond character in C-N bond. Vibrational bands for silatrane moiety remained unaffected after complexation. All the bands observed for silatranyl moiety are consistent with literature in addition to Si-N bond observed in the region 584–576 cm^{-1}.

NMR spectroscopy

^1H and ^{13}C NMR chemical shifts studied for molecular structure were obtained by HF and DFT (B3LYP) and compared with experimental NMR data. GIAO ^1H and ^{13}C chemical shifts values (with respect to TMS) were obtained at HF/3–21G*(d), HF/6–31+G(d), B3LYP/3–21G*(d), and B3LYP/6–31+G(d)

TABLE 4
Comparison of observed FT-IR and calculated frequencies of **2** (HF and DFT methods) along with their probable assignments

>HF	DFT	Exp. Value	Assignments
6–31+G (d)	6–31+G (d)		
3383	3407	3378 s (b)	ν_{as} (N-H)
3314	3330		ν_{s} (N-H)
2929–2910	2986–2965		ν_{as} (NCH_2) and ν_{as} (OCH_2)
2903	2973		ν_{as} (CCH_2C)
2872–2869	2909–2906		ν_{s} (OCH_2)
2839–2835	2889–2886	2934.6 vs 2875.9 vs	ν_{s} (NCH_2)
1620	1611	1630.5 m	ρ (N-H)
1616	—		ρ (N-H)
1534	1506	1532.1 s	ω (NH_3)
1469	1464	1471.5 vs	δ (H_3NCH_2)
1458	1458		δ (CCH_2C)
1428	1423	1414.6 w	δ ($SiCH_2$)
1367	1369	1378.0 s	ω (OCH_2)
1361	1352	1326.6 s	ω (CH_2CH_2C)
1290	1275	1279.3 vs	t (CCH_2C)
1142	1110	1192.6 m	ν_{as} (Si-O)
1119	1088	1124.0 vs	ν (C-O)
1055	1160	1096.8 vs	ν_{as} (NC_3)
1016	1068	1016.7 s	ν (C-C) chain
976	972	971.5 w	ν_{s} (NC_3)
958	1008	938.8 s	ν (C-C) ring
833	967	909.3 s	ν (C-N) ring
768	747	762.8 vs	ν_{s} (Si-O)
706	760	721.1 vs	ν (Si-C)
595	578	583.4 s	ν (Si-N)

Note. s = strong; m = medium; w = weak; νas = asymmetric stretching; νs = symmetric stretching; δ = in–plane bending; ω = out–of–plane bending; ρ = scissoring; t = twisting.

TABLE 5
Antibacterial screening data for **4** (inhibition zone diameter after 12 h)

	Inhibition zone diameter (mm)		
Compound	***E. coli***	***Bacillus subtillus***	***Staphylococcus aureus***
Compound 4	9	9	10
Ampicillin (10 μg/mL)	52	52	46

TABLE 6
In vitro antibacterial activity of compound **4** bacterial strain of *Bacillus subtillus* using microbroth dilution assay

	MIC_{50} (mg/mL)	MIC_{90} (mg/mL)	MIC range (mg/mL)
Compound 4	1.8	3.9	0.8–3.94
Ampicillin	0.00004	0.0001	0.00002–0.0001

levels of theory for the optimized geometries. ^{13}C chemical shift values obtained with HF/3–21G*(d) were found to be different from the values obtained from other studies: HF/6–31+G*(d), B3LYP/3–21G*(d), and B3LYP/6–31+G*(d), which are found to be consistent with experimental values. Comparing ^{1}H NMR spectra of **2** with those of **1**, a downfield shift was observed for $CH_2(\beta)$ and $CH_2(\gamma)$. It may be attributed to the presence of electron withdrawing Cl^- adjacent to $CH_2(\gamma)$. In addition, a singlet observed at 1.9 ppm due to NH_2 in **1** disappeared and a singlet at 7.2 ppm for NH_3^+ protons appeared in **2** indicated the formation of ammonium salt.

^{1}H NMR spectra of **4** shows a downfield shift for OCH_2 (3.75–3.78 ppm) and NCH_2 (2.80–2.83 ppm) protons of $Si(OCH_2CH_2)_3N$ moiety as compared with precursor **1**. Correspondingly, triplet due to -CH_2NCS_2 protons is also shifted downfield as compared to –CH_2NH_2. Comparison of NMR data with previously reported 3-isothiocyanatopropylsilatrane showed that peaks due to -CH_2NCS_2 and -CCH_2C- are shifted downfield, whereas there is no significant change in the positions of other peaks. This indicates that silatranyl moiety is not affected by the presence of different groups on C3 (NCS or NCS_2) due to the presence of bridge formed by -$CH_2CH_2CH_2$- chain. In the ^{13}C NMR, δ NCS_2 appeared at 209.41 ppm, which is shifted downfield as compared with δ NCS (177.05 ppm) in 3-isothiocyanatopropylsilatrane. The peaks appearing at 55.0 and 48.0 ppm due to δ OCH_2 and NCH_2 are observed at the same position as in **1**.

UV-vis spectra

UV-vis absorption spectra, recorded in chloroform for all compounds (**4–8**), confirm the formation of metal complexes. Absorption spectra for **4** showed maxima at 254 and 287 nm,

TABLE 7
In vitro antibacterial activity of compound **4** bacterial strain of *Escherichia coli* using microbroth dilution assay

	MIC_{50} (mg/mL)	MIC_{90} (mg/mL)	MIC range (mg/mL)
Compound 4	1.7	3.6	0.765–3.62
Ampicillin	0.00004	0.0001	0.00002–0.0001

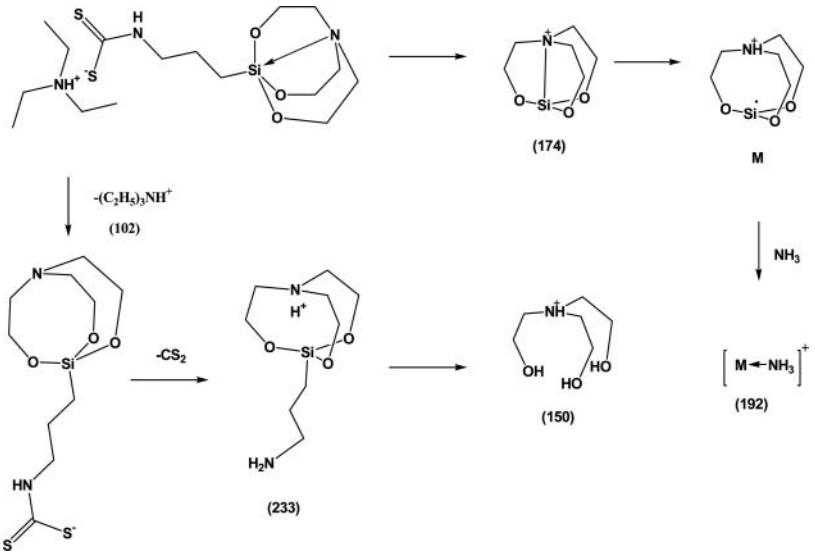

SCH. 3.

whereas all metal complexes were colored and showed maxima in visible region due to d-d transitions. The expected structures for these metal complexes are shown in Figure 4, which are in accordance with the literature.[21,22]

Mass spectra

Mass spectral data of **4** shows characteristic fragmentation pattern of silatrane moiety. A base peak due to $(C_2H_5)_3NH^+$ was observed at m/e = 102. The presence of a peak due to silatranyl cation at 174 is a very common feature in the mass spectrum of silatranes, which is formed by the homolytic cleavage of Si-CH_2 bond. The stability of silatranyl cation has been discussed on the basis of theoretical studies.[23] A peak observed at m/e 233 is assigned to fragment formed by the removal of CS_2 and triethylammonium ion from **4**. In addition, silatranyl moiety undergoes fragmentation and shows peaks at m/e value 150 and 192 as shown in Scheme 3.

Biological Activity

To find out antibacterial activity, compound **4** was dissolved in DMSO and the sample was tested in triplicate. DMSO alone was taken as control and results were compared with control. Antibacterial activity is classified as highly active (>14 mm), moderately active (10–14 mm), slightly active (6–10 mm), and less than 5 mm is taken as inactive. Data of antibacterial activity are shown in Table 5.

The minimum inhibitory concentrations (MIC) of compound **4** were determined by using microbroth dilution method. In the broth dilution MIC method, various concentrations of a compound were inoculated with a standard suspension of test bacteria. Following an overnight incubation at 35°C, MIC was determined by observing lowest concentration of the compound that will inhibit visible growth of the test bacteria. Growth was determined photometrically by measuring A_{600}. Percentage of growth was calculated by using the following formula:

$$\text{Percentage of growth} = \frac{\text{OD of organism grown with sample}}{\text{OD of control}}$$

MIC data against bacterial culture of *Bacillus subtillus*, *Escherichia coli*, and *Staphylococcus aureus* is summarized in Tables 6, 7, and 8, respectively. MIC_{50} (defined as minimum concentration at which 50% of the isolates were inhibited) of compound **4** against *Bacillus subtillus* was 0.0382 mg/mL, whereas MIC_{90} (defined as minimum concentration at which 90% of the isolates were inhibited) was 0.0689 mg/mL.

TABLE 8
In vitro antibacterial activity of compound **4** bacterial strain of *Staphylococcus aureus* using microbroth dilution assay

	MIC_{50} (mg/mL)	MIC_{90} (mg/mL)	MIC range (mg/mL)
Compound 4	1.5	3.2	0.625–3.21
Ampicillin	0.00005	0.00015	0.00003–0.0001

Note. Ampicillin has been used as standard drug.

CONCLUSION

The present work summarizes crystallographic, theoretical, and spectroscopic data of 3-(silatranyl)propylammonium chloride. The formation of **2** is attributed to photochemical reaction of **1** in dichloromethane. X-ray crystal structure parameters are in accordance with theoretical studies. It is also concluded that 3-aminopropylsilatrane undergoes 1:1 addition reaction with CS_2 to form 3-siltranylpropyldithiocarbamic acid, which can

yield triethylammonium-3-silatranylpropyldithiocarbamate on treatment with triethylamine. The product was obtained in very good yield and spectroscopic data have shown characteristics of dithiocarbamate as well as silatranyl moiety. Dithiocarbamate moiety shows chelation with different transition metal ions due to the presence of S atoms. Spectral results support proposed structures of the metal complexes. In addition, antimicrobial activity of newly synthesized compound **4** was also evaluated against bacterial culture of *Bacillus subtillus*, *Escherichia coli*, and *Staphylococcus aureus.* The results obtained clearly indicate that compound **4** discussed here is active toward growth inhibition of bacteria under this investigation.

SUPPLEMENTARY MATERIALS

CCDC 738531 contains the supplementary crystallographic data for this paper. These data can be obtained free of charge from The Cambridge Crystallographic Data Centre via www.ccdc.cam.ac.uk/data_request/cif. Spectroscopic data and theoretical data of synthesized molecules are given in supporting information.

REFERENCES

1. Voronkov, M.G.; Dyakov, V.M.; Kirpichenko, S.V. *J. Organomet. Chem.* **1982**, *233*, 1.
2. Pestunovich, V.; Kirpichenko, S.; Voronkov, M.G. In *Chemistry of Organic Silicon Compounds*, Rappoport, Z., Apeloig, Y., eds. Wiley: Chichester, England, **1998**.
3. Chuit, C.; Corriu R.J.P.; Reye, C.; Young, J.C. *Chem. Rev.* **1993**, *93*, 1371.
4. Puri, J.K.; Singh, R.; Chahal, V.K.; *Chem. Soc. Rev.* **2011**, 40, 1791.
5. Singh, R.; Puri, J.K.; Chahal, V.K.; Sharma, R.P.; Venugopalan, P. *J. Organomet. Chem.* **2010**, *695*, 183.
6. Li, Z.; Tian, D.; Zhu, C. *Phosphorus, Sulfur Silicon Relat. Elem.* **2000**, *165*, 99.
7. Li, Z.; Tian, D. *Heterocycl. Commun.* **2003**, *9*, 605.
8. Tharmaraj, P.; Kodimunthiri, D.; Sheela, C.D.; Priya, C.S. S. *J. Coord. Chem.* **2009**, *62*, 2220.
9. Puri, J.K.; Singh, R.; Chahal, V.K.; Sharma, R.P. *ARKIVOC*, **2009**, *xi*, 247.
10. Singh, R.; Puri, J.K.; Sharma, R.P.; Malik, A.K.; Ferretti V. *J. Mol. Struc.* **2010**, *982*, 107.
11. Puri, J.K.; Singh, R.; Chahal, V.K.; Sharma, R.P.; Wagler, J.; Kroke, E. *J. Organomet. Chem.* **2011**, *696*, 1341.
12. Bond A.M.; Martin, R.L. *Coord. Chem. Rev.* **1984**, *54*, 23.
13. Coffey, T.A.; Foster, G.D.; Hogarth, G. *J. Chem. Soc., Dalton Trans.* **1996**, *2*, 183.
14. *CrysAlis^{Pro}, Data collection and Processing Software*; Oxford Diffraction Limited: Oxford, England.
15. Wan, S.G.; Yang, X.Y.; Yu, Y.; Liu, C. *Phosphorus, Sulfur Silicon Relat. Elem.* **2005**, 180, 2813.
16. Balsells, R.E.; Frasca, A.R. *Aus. J. Chem.* **1988**, *41*, 103.
17. Attar-Bashi, M.T.; Rickard, C.E. F.; Roper, W.R.; Wright, L.J.; Woodgate, S.D. *Organometallics*, **1998**, *17*, 504.
18. Duax, W.L.; Norton, D.A. *Atlas of Steroid Structure*; Plenum: New York, **1975**.
19. Duax, W.L.; Weeks, C.M.; Roherer, D.C. *Topics of Stereochemistry*, Vol. 9; Wiley: New York, **1976**.
20. Herring, F.G.; Parks, J.M.; Rettig, J.; Trotter, J. *Can. J. Chem.* **1979**, *57*, 2379.
21. Zhang, J.; Jian, F.; Lu, L.; Yang, X.; Wang, X. *J. Chem. Crystallogr*. **2001**, *31*, 251.
22. Jian, F.; Bei, F.; Zhao, P.; Wang, X.; Fun, H.; Chinnakali, K. *J. Coord. Chem.* **2002**, *55*, 429.
23. Lee, H.S.; Bae, C.; Do, Y.; Lee, Y.S. *Bull. Korean Chem. Soc.* **2002**, *23*, 215.